JACS
JOURNAL OF THE AMERICAN CHEMICAL SOCIETY

Article

pubs.acs.org/JACS

# Evaluation of Hydrogen-Bond Acceptors for Redox-Switchable Resorcin[4]arene Cavitands

Igor Pochorovski, Jovana Milić, Dušan Kolarski, Cornelius Gropp, W. Bernd Schweizer, and François Diederich*

Laboratorium für Organische Chemie, ETH Zürich, Hönggerberg, HCI, 8093 Zürich, Switzerland

Supporting Information

**ABSTRACT:** Various H-bond acceptor groups were evaluated for their propensity to induce conformational switching between the kite and vase forms of diquinone-diquinoxaline resorcin[4]arene cavitands upon redox interconversion. The H-bond acceptors were placed on the quinoxaline walls with the purpose of stabilizing the vase form only in the reduced hydroquinone state of the cavitand by forming H-bonds with the hydroquinone OH groups. Design guidelines for successful acceptors were derived. The carboxamide acceptor was shown to be the best candidate. Based on this moiety, a redox-switchable triptycene-based basket that can completely sterically encapsulate a guest in its closed vase conformation was prepared. The basket binds small molecule guests with association constants of up to $10^4$ $M^{-1}$ in mesitylene-$d_{12}$ and exhibits slow guest exchange kinetics with a half-life for guest release in the order of $10^4$ s.

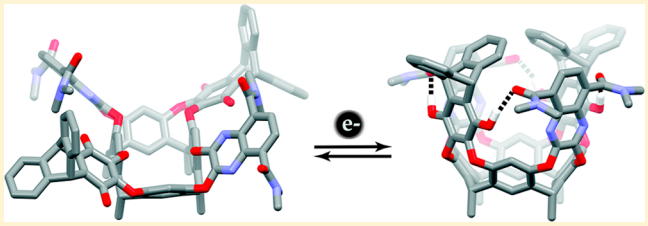


## INTRODUCTION

Every rationally designed molecular machine,[1] whose behavior is studied and discerned, expands the boundaries of our understanding of the molecular world and further transforms the field of supramolecular chemistry from science to engineering. The resorcin[4]arene cavitand system is an intriguing platform for designing molecular machines, because it can adopt two spatially distinct forms: an expanded "kite" and a contracted "vase."[2] Switching between the two forms can be employed to grab and release small molecules, enabling the application of cavitands as molecular grippers.[3] Besides the ability to switch the properties of cavitands[4] using stimuli such as changes in temperature,[2,5] pH,[6] metal ion concentration,[7] or light,[8] our recently introduced concept for the design of redox-switchable cavitands[9] (Figure 1A) is particularly promising for the application of cavitands in electronic devices, as redox-switchable derivatives have the potential to be interfaced with electroactive metal surfaces.[10]

The switching concept is based on H-bonding interactions that stabilize the vase form and are only present in the reduced hydroquinone state of the cavitand. Assuming that the H-bond strength influences the switching ability and binding properties,[9b,11] we sought to investigate various H-bond acceptor groups[12] on the basis of the ester- (**1**), pyridine- (**2**–**4**), imidazole- (**5**), and carboxamide-based (**6**)[13] cavitands (Figure 1B). The results of this study are presented herein. We established that the carboxamide moiety in cavitand **6** is best suited for assisting redox-induced conformational switching. Guided by this finding, we prepared the redox-switchable basket system **7**, which can completely encapsulate guests in its vase conformation due to the triptycene walls.[14] The reduced basket red-**7** exhibited high association constants ($K_a$ in the range of $10^2$–$10^4$ $M^{-1}$) for suitably sized guests in mesitylene-$d_{12}$ and slow guest release kinetics with a half-life $\tau_{1/2}$ in the order of $10^4$ s.

## RESULTS AND DISCUSSION

**Synthesis.** The syntheses of cavitands ox-**1** and ox-**3**–**7** commenced with the preparation of wall precursors **8**–**13** (Scheme 1A). Precursor **8**[15] and **9a**[9b] were accessed according to literature procedures. Precursor **10** was prepared from diboronic ester **14**.[16] In the first step, **14** and 2-bromopyridine were reacted in a Suzuki cross-coupling to yield benzothiadiazole **15**. In the next steps, reductive sulfur extrusion,[17] condensation of the resulting diamine with oxalic acid,[18] and chlorination of the resulting diol intermediate[18] yielded precursor **10**. Precursor **11** was prepared from compound **16**, employing the same three-step procedure described above. Compound **16**, in turn, was obtained in a one-pot sequence from 1-octylimidazole (**17**)[19] *via* stannylation to stannane **18** and Stille coupling with dibromide **19**. Precursors **12** and **13** were accessed from compound **20**[20] and pyrazines **21**[21] and **22**,[21] respectively. Toward precursor **9b**, dibromide **19** was reacted in a Pd-catalyzed aminocarbonylation reaction[22] with $n$Bu$_2$NH and CO, affording compound **23**. Reductive sulfur extrusion from **23**,[17] condensation of the resulting diamine with oxalic acid,[18] and chlorination of the resulting diol with thionyl chloride[18] then yielded precursor **9b**.

**Received:** November 9, 2013
**Published:** February 25, 2014

   dx.doi.org/10.1021/ja411429b | J. Am. Chem. Soc. 2014, 136, 3852–3858

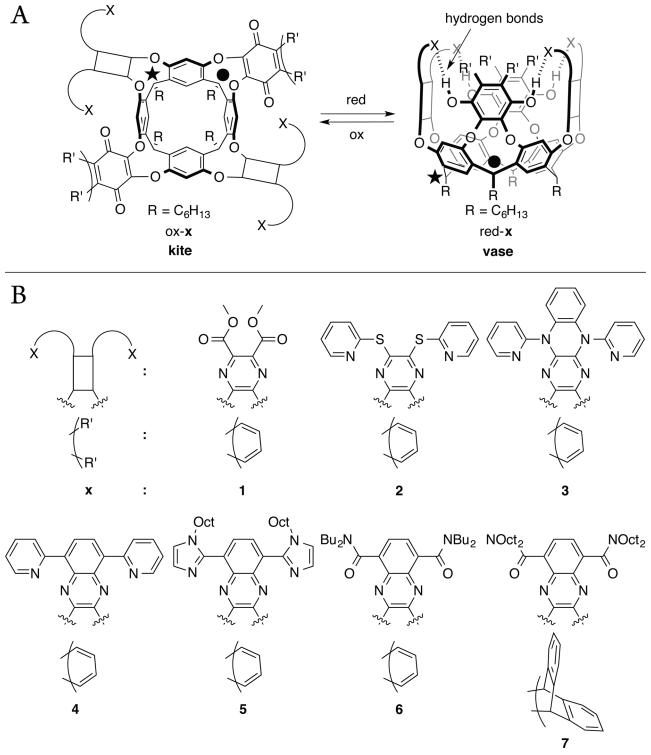


**Figure 1.** (A) Design concept of redox-switchable cavitands (X = H-bond acceptor; the symbols ● and ★ represent methine protons). (B) Target cavitands in this study.

Subsequently, we proceeded with the assemblies of cavitands ox-**1**−**7** (Scheme 1B). Cavitands ox-**1** and ox-**4**−**6** were prepared through condensations of tetrol **24**[9b,23] with precursors **8**−**11**, respectively. The synthesis of cavitand ox-**2** required a different strategy, because the respective wall precursor analogous to **8**−**13** is not easily accessible. Hence, we planned to prepare cavitand ox-**2** *via* nucleophilic substitution reaction between the difluoropyrazine-substituted cavitand **25**, which was prepared from tetrol **24** and pyrazine **22**, and pyridine-2-thiol (**26**).[24] This reaction did not, however, yield cavitand ox-**2** directly. Instead, **26** caused the excision of quinone walls to yield intermediate **27** (as revealed by MALDI-MS). This observation means that the quinone walls of **25** are more reactive toward nucleophilic attack than C−F bonds on the pyrazine rings. Nevertheless, the desired cavitand ox-**2** was obtained by transforming intermediate **27** into **28** with an excess of **26**, and reattaching the quinone walls with compound **29**. The synthesis of cavitand ox-**3** was attempted *via* two different routes: (i) reaction of compound **20** and cavitand **25** and (ii) reaction of tetrol **24** with dichloropyrazine **12** or difluoropyrazine **13**. However, neither of the routes was successful. The outcome of route i was quinone excision instead of substitution of the fluorine atoms, while in route ii neither **12** nor **13** was reactive with tetrol **24**. Presumably, the electron-donating dihydropyrazine-*N*-atoms strongly reduce the reactivity of the pyrazine C−Cl bonds (in **12**) and the C−F bonds (in **13**) in nucleophilic substitution reactions. Basket ox-**7** was obtained by condensing precursor **9b** with tetrol **30**.[9b]

With the oxidized cavitands in hand, we continued with accessing their reduced redox states (Scheme 1C). Cavitands red-**1**−**2** and red-**4**−**6** were obtained through reductions of ox-**1**−**2** and ox-**4**−**6** with $Na_2S_2O_4$ in biphasic mixtures of $CDCl_3$/$H_2O$. When the reductions were finished, the $CDCl_3$ layers were transferred into $N_2$-filled NMR tubes containing ∼5 mg of anhydrous $MgSO_4$ (in order to remove traces of $H_2O$) and analyzed by $^1$H NMR. The oxidized states could be regenerated upon exposing the cavitand solutions to air for 2−4 d. The reduced basket red-**7** was obtained from ox-**7** through reduction with Pd/C under a $H_2$ atmosphere in THF. Triptycenequinone-based basket red-**7** is more stable toward oxidation by air oxygen compared to the naphthoquinone-based cavitands red-**1**−**2** and red-**4**−**6** (in the solid state for at least 2 months). Oxidation of red-**7** to ox-**7** could, however, be achieved by exposing a chloroform solution of red-**7** to air for ∼7 d.

**X-ray Structures of Wall Precursor 12 and Cavitand ox-4.** Crystals of precursor **12** suitable for X-ray analysis were obtained by evaporation from a $CHCl_3$/EtOH solution. The molecular structure of **12** in the crystal is shown in Figure 2 (left). The torsion angle of the pyridine plane relative to the main molecular plane is 78°, which would position the pyridine acceptor in an optimal orientation for H-bonding with the hydroquinone OH groups if the unit was incorporated into a cavitand system. Crystals of cavitand ox-**4** were obtained by evaporation from a MeCN/$CH_2Cl_2$ solution (Figure 2, right). The cavitand crystallized in the kite conformation, which is typical for diquinone-diquinoxaline cavitands.[9a] The pyridine N atoms are oriented away from the platform in order to avoid lone pair repulsion with the N atoms of the quinoxaline moieties. Although the kite form should have $C_{2v}$ symmetry, it does not in the crystal; the pyridine moieties that are in the vicinity of the quinone units adopt torsion angles of 154−158° relative to the quinoxaline walls, while the ones that are further away adopt torsion angles of 130−138°.

**Conformational Properties of Cavitands ox-1−2 and ox-4−6, and red-1−2 and red-4−6 Studied by $^1$H NMR Spectroscopy.** The ability of the various H-bond acceptor groups in cavitands ox-**1**−**2** and ox-**4**−**6** to assist conformational switching upon redox interconversion was investigated by $^1$H NMR spectroscopy. Figure 3 (left) shows the $^1$H NMR spectra of the oxidized cavitand states in $CDCl_3$. The adopted conformations, kite or vase, are revealed by the characteristic resonances of the methine protons (● and ★, denoted in Figure 1A).[2] Details about the assignment of the resonances (● or ★) to the corresponding methine protons (the ones below the quinone or quinoxaline walls) are presented in the Supporting Information, section 3.3. For all cavitands, the methine protons are located between 3.6 and 4.4 ppm, indicating the presence of the kite conformations in the oxidized cavitand states.[2] This finding is in line with the fact that (unsubstituted) diquinone-diquinoxaline cavitands favor the kite over the vase form in chlorinated solvents.[9a]

$^1$H NMR spectra of the reduced cavitands red-**1**−**2** and red-**4**−**6**, on the other hand, reveal pronounced differences (Figure 3, right). The ester-substituted red-**1** is present in the kite form (methine protons at 3.4 and 4.5 ppm), which means that conformational switching upon redox interconversion does not take place in that system. On the other hand, the methine protons of the *S*-pyridine-substituted cavitand red-**2** resonate at 5.4 and 5.6 ppm. Although these signals are broad, indicating a dynamic structure, their position testifies that red-**2** adopts the vase conformation. Surprisingly, the $^1$H NMR spectra of pyridine-substituted cavitand red-**4** and imidazole-substituted cavitand red-**5** displayed very broad peaks, over a wider temperature range, allowing no direct conclusion about the


dx.doi.org/10.1021/ja411429b | J. Am. Chem. Soc. 2014, 136, 3852−3858

**Scheme 1. Synthetic Routes Towards Cavitands ox-1−7 and red-1−7**[a]

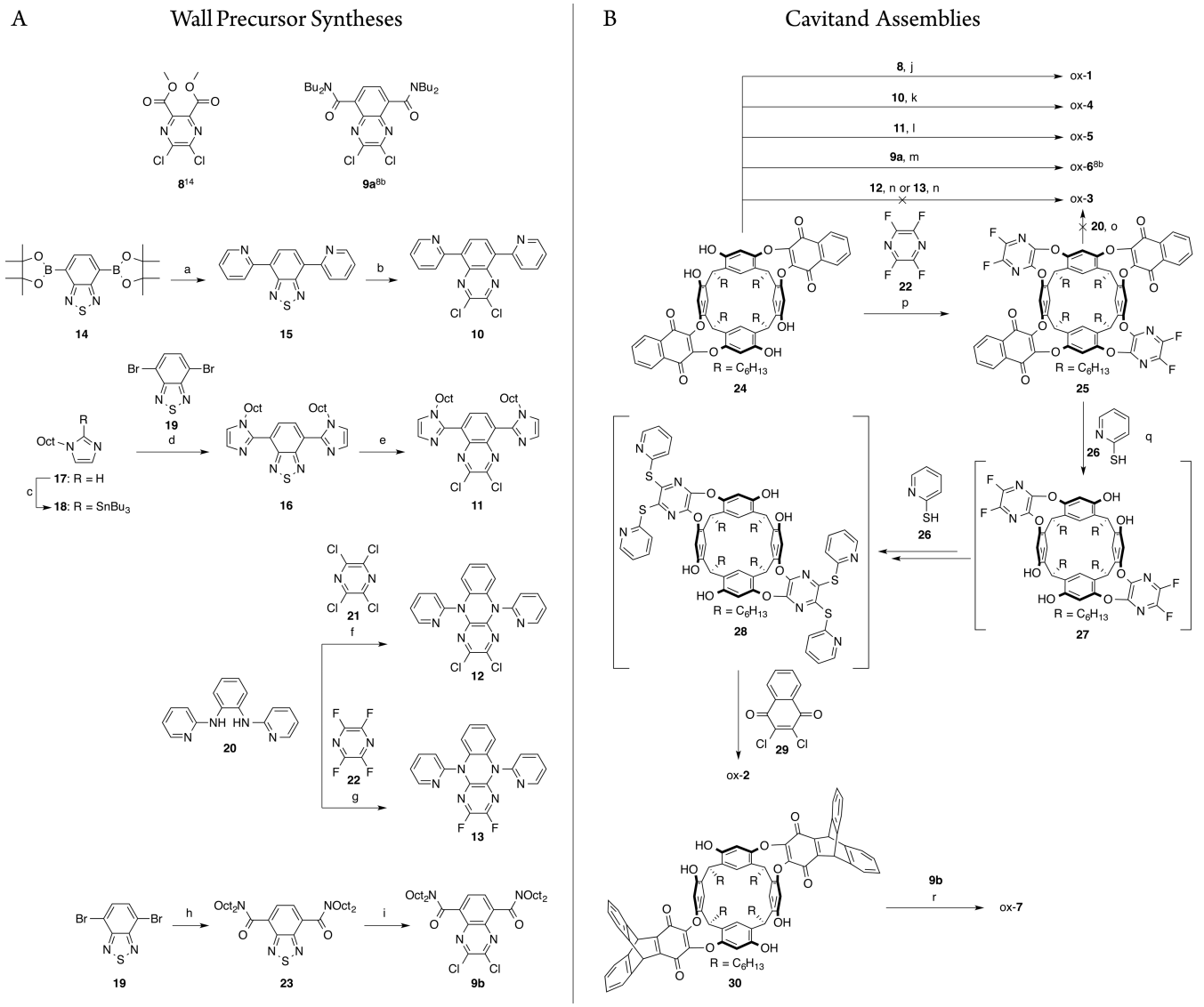


[a](a) 2-Bromopyridine, $K_2CO_3$, $[Pd(PPh_3)_4]$, toluene/$H_2O$, 80 °C, 48 h; 71%. (b) (1) $NaBH_4$, $CoCl_2{\cdot}6\ H_2O$, EtOH, reflux, 30 min; (2) $(COOH)_2$, 4 M HCl, 100 °C, 15 h; (3) $POCl_3$, DMF, 100 °C, 15 h; 69%. (c) (1) *n*BuLi, THF, −78 °C, 1 h; (2) $nBu_3SnCl$, THF, 0→25 °C, 12 h. (d) $[Pd(PPh_3)_4]$, THF, reflux, 72 h; 21%. (e) (1) $NaBH_4$, $CoCl_2{\cdot}6\ H_2O$, EtOH, reflux, 3 h; (2) $(COOH)_2$, 4 M HCl, 100 °C, 12 h; (3) $SOCl_2$, DMF/$(CHCl_2)_2$, 100 °C, 4 h; 10%. (f) $Cs_2CO_3$, DMF, 120 °C, 16 h; 59%. (g) $Cs_2CO_3$, DMF, 90 °C, 5 h; 57%. (h) $nOct_2NH$, CO (balloon), $[Pd(OAc)_2]$, Xantphos, $K_3PO_4$, toluene, reflux, 3 d; 78%. (i) (1) $NaBH_4$, $CoCl_2{\cdot}6\ H_2O$, EtOH, reflux, 6 h; (2) $(COOH)_2$, EtOH/HCl, reflux, 4 d; (3) $SOCl_2$, DMF, $(CH_2Cl)_2$, 100 °C, 16 h; 40%. (j) $Cs_2CO_3$, THF, 50 °C, 3 h; 68%. (k) $Cs_2CO_3$, THF, reflux, 12 h; 28%. (l) $Cs_2CO_3$, DMF, 25 °C, 4 h; 27%. (m) $Cs_2CO_3$, THF, reflux, 24 h; 85%. (n) $Cs_2CO_3$, DMF, 70 °C, 12 h. (o) $Cs_2CO_3$, DMF, 50 °C, 12 h. (p) $K_2CO_3$, DMF, 0→25 °C, 16 h; 50%. (q) (1) **26**, $Cs_2CO_3$, DMF, 50 °C, 9 h; (2) **29**, $Cs_2CO_3$, DMF, 50 °C, 13 h; 9%. (r) $Cs_2CO_3$, THF, reflux, 16 h; 29%. (s) $Na_2S_2O_4$, $CDCl_3/H_2O$, 60 °C, 3 h, quantitative. (t) Air, $CDCl_3$, quantitative. (u) $H_2$, Pd/C, THF, 25 °C, 3 h, quantitative. (v) Air, $CDCl_3$, quantitative.

adopted conformations of these cavitands. Decompositions were ruled out, as cavitands ox-**4** and ox-**5** fully regenerated upon exposing the solutions of red-**4** and red-**5** to air for 1−3 d. In contrast, the $^1$H NMR spectrum of red-**6** displays sharp


dx.doi.org/10.1021/ja411429b | J. Am. Chem. Soc. 2014, 136, 3852−3858

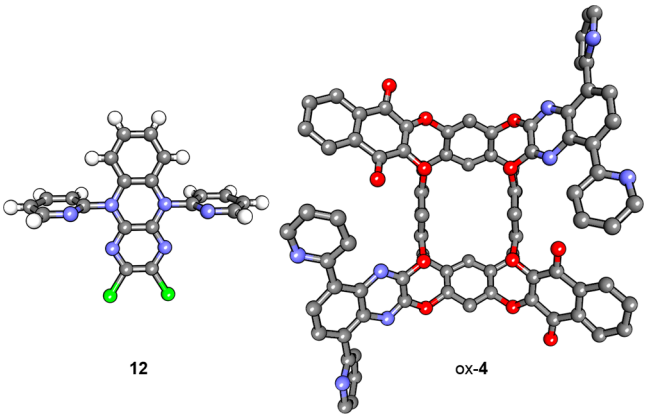


**Figure 2.** Molecular structures of wall precursor **12** and cavitand ox-**4** in their respective crystals at 100 K. Crystals of **12** were obtained from $CHCl_3$/EtOH and those of ox-**4** from $CH_2Cl_2$/MeCN. In case of ox-**4**, solvent molecules, *n*-hexyl chains, and H-atoms are omitted for clarity.

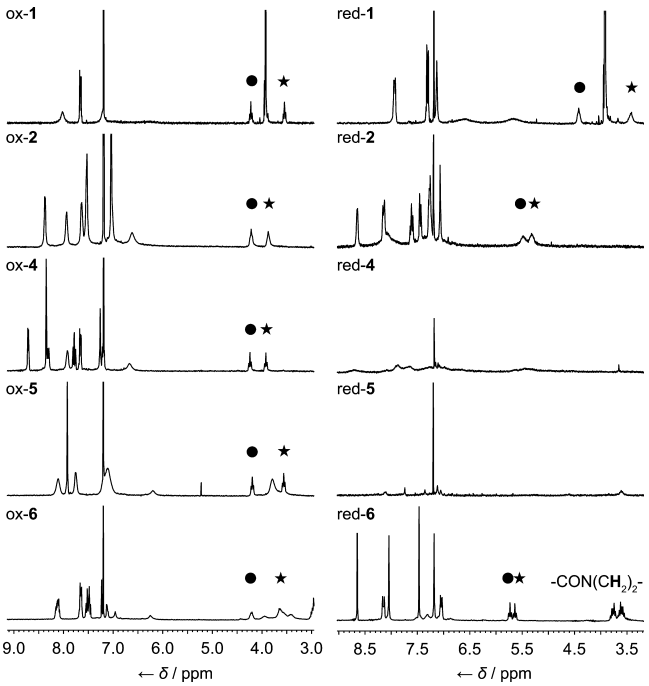


**Figure 3.** Sections of the $^1$H NMR spectra (298 K) of cavitands ox-**1**−**2** and ox-**4**−**6**, and red-**1**−**2** and red-**4**−**6** in $CDCl_3$ (300 MHz). The symbols ● and ★ represent methine protons; for assignment, see Figure 1A.

triplets for the methine protons located at 5.7 and 6.2 ppm, indicating the presence of a rigid vase conformation.[9b]

Baskets ox-**7** and red-**7** exhibit the same conformational properties as cavitands ox-**6** and red-**6**; ox-**7** is present in the kite conformation in $CDCl_3$ (methine protons between 3.8 and 4.2 ppm), while red-**7** adopts a rigid vase form (methine protons at 5.6 and 5.7 ppm as sharp triplets).[25]

**Computational Studies.** In order to rationalize the conformational properties of cavitands red-**1**−**2** and red-**4**−**6** discussed above, we computed their optimized structures with DFT at the B3LYP/6-31G(d) level of theory (Figure 4, alkyl chains were exchanged by methyl groups).[26] In the ester-based cavitand red-**1**, only one COOMe group per bis(COOMe) unit can participate in H-bonding with the hydroquinone OH groups due to steric reasons. Consequently, only two

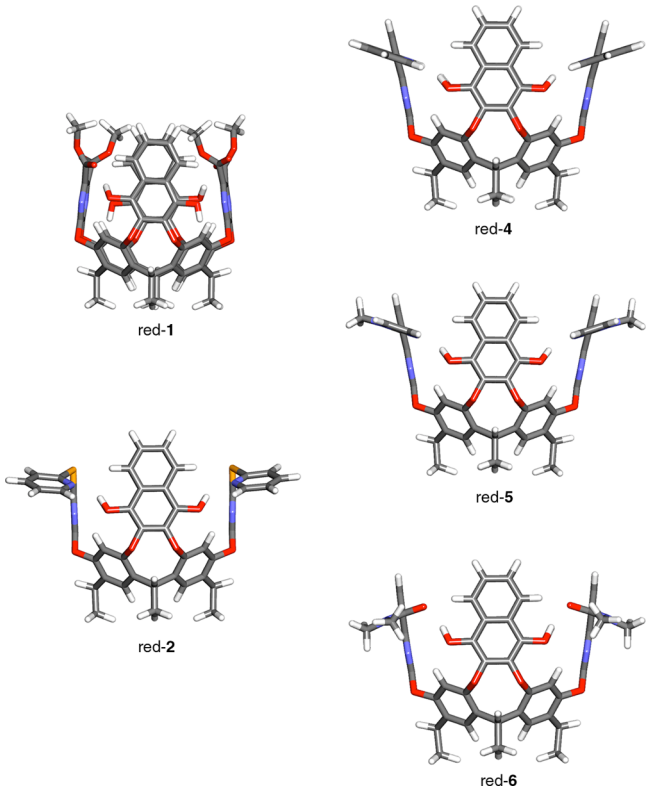


**Figure 4.** Structures of cavitands red-**1**−**2** and red-**4**−**6** optimized at the DFT B3LYP/6-31G(d) level of theory. Alkyl chains were exchanged by methyl groups.

hydroquinone OH groups per cavitand undergo H-bonding with the weak[12] COOMe H-bond acceptors, while the other two establish H-bonds with the ether oxygen atoms of the cavitand backbone. On the other hand, in cavitand red-**2** the formation of all four H-bonds between the pyridine and hydroquinone OH groups is possible. These observations are in line with $^1$H NMR results, according to which red-**1** adopts the kite and red-**2** the vase form (Figure 3, right). Apparently, the formation of only two H-bonds is not sufficient to stabilize the vase form but formation of all four is required. While all four H-bonds can, in principle, be established in case of cavitands red-**4**−**6** (Figure 4), only red-**6** clearly adopts a vase conformation according to $^1$H NMR spectroscopy (Figure 3, right).

To understand why red-**6** adopts the vase form while red-**4** and red-**5** do not, we performed dihedral angle ($\theta$) scans between the pyridine, imidazole, and carboxamide moieties, respectively, and the quinoxaline moieties of hypothetical test systems shown in Figure 5. The calculations were performed at the MP2/cc-pVTZ//B3LYP/6-31+G(d,p)[27] level of theory. The global energy minima are located at dihedral angles of 140° for the pyridine-wall model (which is consistent with the dihedral angle range of 130−158° observed in the crystal structure of ox-**4**, Figure 2), 130° for the imidazole-wall model, and 120° for the carboxamide-wall model. However, formation of intramolecular H-bonds in the hydroquinone cavitands is structurally only possible for dihedral angles $\theta$ in the range of 60−100°. Turning the moieties into this desired $\theta$ range requires at least 1.9 kcal mol$^{-1}$ for the pyridine, 1.3 kcal mol$^{-1}$ for the imidazole, and 0.3 kcal mol$^{-1}$ for the carboxamide moiety. Thus, in case of the pyridine and imidazole moieties, the energetic cost for this process is presumably larger than that of remaining in the optimal orientations and establishing


dx.doi.org/10.1021/ja411429b | J. Am. Chem. Soc. 2014, 136, 3852−3858

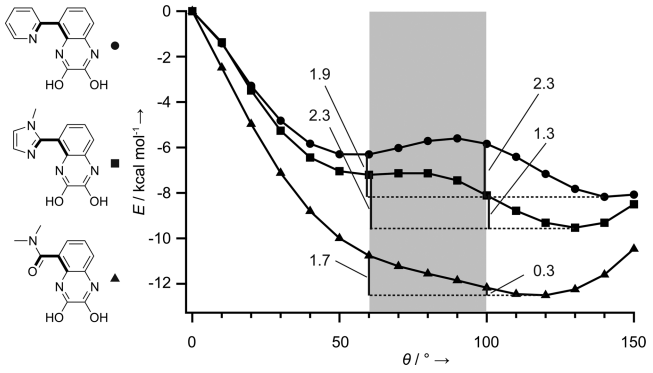


**Figure 5.** Dihedral angle scans for hypothetical test systems containing the pyridine, imidazole, and carboxamide moieties, performed on the MP2/cc-pVTZ//B3LYP/6-31+G(d,p) level of theory. The highlighted gray area is the dihedral angle range, in which H-bonding to the hydroquinone OH groups would be possible in the cavitand systems.

intermolecular H-bonds with OH groups of other cavitand molecules. On the other hand, the low barrier in the case of the carboxamide moiety is smaller than the entropic costs of intermolecular aggregations. This rationale is in line with the complex $^1$H NMR spectra of red-**4** and red-**5** (Figure 3, right) that could be explained by aggregate formation based on intermolecular H-bonds,[28] and the $^1$H NMR spectrum of red-**6** that reveals a rigid vase conformation stabilized by intramolecular H-bonds.[9b]

**Binding Properties of Baskets ox-7 and red-7.** In our earlier communication[9b] we showed that the top-open H-bond-stabilized cavitand red-**6** binds alicyclic guests with association constants $K_a$ in the range of $10^1$−$10^3$ $M^{-1}$, and guest release rates with a half-life $\tau_{1/2}$ in the order of $10^{-2}$ s. With the basket system ox-/red-7 we sought to investigate whether the sterically congesting triptycene moiety can further enhance the association constants and slow down guest release.

The binding studies were performed in mesitylene-$d_{12}$, as this solvent is too large to compete with guests for the cavitand binding site. In mesitylene-$d_{12}$, ox-7 is present in the kite and red-7 in the vase conformation. Thus, while red-7 was already preorganized for binding, ox-7 switched from kite to vase upon guest uptake (see Figures S6 and S7 in the Supporting Information). One aspect complicating binding studies with red-7 was that THF, which was used as solvent during the reduction of ox-7 to red-7, remained tightly bound by the cavitand.[29] Difficulties to remove residual solvent from cavitands with strong binding properties have already been reported.[6b,c,30] Therefore, binding studies with red-7 were performed with samples containing 0.4 equiv of THF, whereby the association constants were corrected for the presence of THF as a competing guest.[31] The association constants between cavitands ox-7 and red-7 and various guests are shown in Table 1. The $K_a$ values of red-7 are significantly higher than those of ox-7, by a factor of $10^2$−$10^3$. Within the cycloalkane series, red-7 shows the highest association constant for cyclooctane. Thus, the cavity of red-7 is larger than that of other reported cavitand-based basket systems, which show maxima in $K_a$ for cyclopentane or cyclohexane.[6b,c,30] The largest $K_a$ value was measured for 1,4-cyclohexanedione, presumably due to an optimal size complementarity.[9b]

**Binding Kinetics of Basket red-7.** We investigated the kinetics of guest binding and guest release of the triptycene-derived basket system red-7. While smaller guests reached an equilibrium host−guest concentration directly after guest addition to red-7 and spectrum recording (half-lives of guest uptake $\tau_{1/2}$ < 5 min), the larger cyclooctane exhibited binding kinetics slow enough to be followed by NMR. The concentration vs time curve of the host−guest complex formed between red-7 (∼2 mM) and cyclooctane (∼0.25 equiv) is illustrated in Figure 6 (left). The process followed first-order kinetics, suggesting that the rate-determining step is governed by cavitand opening to an extent at which cyclooctane can slip in. The kinetic and thermodynamic parameters for cyclooctane uptake were determined to be: $k_{in}$ = (5.4 ± 0.3)$10^{-4}$ $s^{-1}$; $\tau_{1/2}$ = 21 ± 1 min; $\Delta G^{\ddagger}_{298\ K}$ = 21.9 kcal $mol^{-1}$. The release kinetics was studied on the example of cyclohexane by monitoring the guest exchange with 1,4-cyclohexanedione − the guest with the highest measured association constant. To a sample containing red-7 (∼1 mM) and cyclohexane (∼1 equiv), an excess (30 equiv) of 1,4-cyclohexanedione was added. The concentration vs time curve of the host−guest complex between cyclohexane and red-7 is illustrated in Figure 6 (right). The exchange process followed first-order kinetics, indicating that the rate-determining step is unimolecular. As the uptake of 1,4-cyclohexanedione was shown to be fast in separate binding experiments ($\tau_{1/2}$ < 5 min), the rate-determining step for the exchange process must be cyclohexane release. The kinetic and thermodynamic parameters for cyclohexane release were determined to be: $k_{out}$ = (5.3 ± 0.2)$10^{-5}$ $s^{-1}$; $\tau_{1/2}$ = 216 ± 7 min; $\Delta G^{\ddagger}_{298\ K}$ = 23.3 kcal $mol^{-1}$.

Guest-exchange mechanisms have been studied for a variety of artificial host systems.[32] The most likely mechanism for guest exchange in cavitands presumably involves two steps:

**Table 1. Association Constants $K_a$ ($M^{-1}$) between Baskets ox-7 and red-7, and Various Guest Molecules (mesitylene-$d_{12}$, 298 K)[a]**

| Guest | | | | |
|---|---|---|---|---|
| $K_a$(ox-7 ⊃guest) / M$^{-1}$ \| $K_a$(red-7 ⊃guest) / M$^{-1}$ | | | | |
|  |  |  |  |  |
| 0.2 \| 160 | 2.6 \| 300 | 8 \| 330 | 2 \| 5300 | 40 \| 8700 |

[a]Determined by integration of the $^1$H NMR resonances of the relevant species, relative to 1,3,5-trimethoxybenzene as internal standard. Errors in $K_a$ are estimated to be 20%. $K_a$ values were corrected to account for the presence of 0.4 equiv THF remaining after reduction in the cavitand sample.

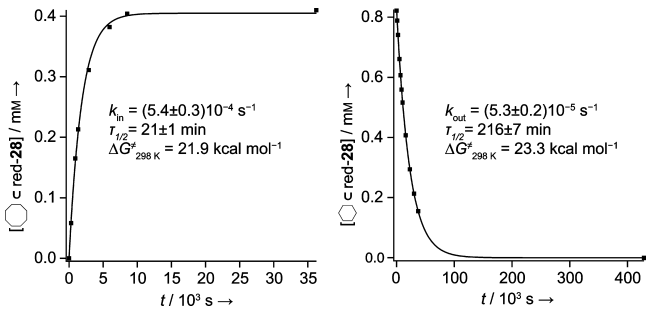


**Figure 6.** (Left) Binding kinetics of cyclooctane by red-7. (Right) Release kinetics of cyclohexane from the host−guest complex with red-7, induced by addition of excess 1,4-cyclohexanedione. Both data sets were treated by a first-order kinetics law with the rate constants as fit parameters.


dx.doi.org/10.1021/ja411429b | J. Am. Chem. Soc. 2014, 136, 3852−3858

dissociation of the leaving guest, followed by association with the incoming guest. The intermediate is presumably not empty but filled with solvent molecules. The transition state is represented by a cavitand structure that is open just to the extent that allows guest release/uptake. The rate-determining step therefore depends on how much the cavitand needs to distort for guest release/uptake to take place, which, in turn, strongly depends on the size of the leaving/incoming guest and the H-bond stabilization energy. Thus, the slow binding kinetics of basket red-**7** is a consequence of both the congesting influence of the triptycene moiety, and the strong hydrogen bonds between the amide and hydroquinone units.

## SUMMARY AND CONCLUSIONS

The goal of this work was to assess the propensity of various H-bond acceptors in assisting conformational switching between the kite and vase forms of diquinone cavitands. We established that all four H-bond acceptors need to be involved in H-bonding with the hydroquinone OH groups in order for the vase form to become energetically favorable. In addition, the acceptor moiety should not have too many conformational degrees of freedom; otherwise the vase form becomes too flexible. Another key design element is to ensure that the optimal dihedral angle of the H-bond acceptor relative to the quinoxaline wall lies within or close to the dihedral angle range of 60−100° in which H-bond formation is sterically possible, or that rotation into this range is accompanied only by a small energetic penalty. A strong H-bond acceptor that is not well preorganized for intramolecular H-bonding will likely rather engage in intermolecular associations. We found that the carboxamide moiety in cavitands red-**6** and red-**7** is an acceptor that excellently satisfies these design guidelines.

Closing the top of red-**6** with the triptycene moiety resulted in a redox-switchable basket **7** with enhanced binding properties in the reduced state compared to the corresponding top-open system.[9b] Association constants in the oxidized state ox-**7** were found to be in the range of $10^{-1}$−$10^{1}$ $M^{-1}$, while association constants in the range of $10^{2}$−$10^{4}$ $M^{-1}$ were measured for the reduced cavitand red-**7**. Thereby, changing the redox state of basket **7** modulates the association constants by a factor of $10^{2}$−$10^{3}$. This switchability of binding properties might eventually allow cavitands of this type to be employed as molecular grippers for nanorobotics. Closing the top of the cavity has furthermore a dramatic impact on guest uptake and release kinetics: the rate constant for cyclooctane uptake by red-**7** was $k_{in} = (5.4 \pm 0.3)10^{-4}$ $s^{-1}$, while that for cyclohexane release was $k_{out} = (5.3 \pm 0.2) \times 10^{-5}$ $s^{-1}$. This rate constant for guest release is significantly lower than those reported for other cavitand systems;[6b,c,9b,11] so far, the record value is $k_{out} = 2.5 \times 10^{-3}$ $s^{-1}$ for the release of a neutral guest (cyclohexane) from a covalently top-bridged cavitand.[6c] Only the covalently bridged carcerands and hemicarcerands can achieve even lower values.[32e,33]

This work is an example of how a molecular system with a desired function can be evolved, with the assistance of molecular design, synthesis, $^{1}$H NMR spectroscopy, X-ray crystallography, and computational studies, from a general concept.

## ASSOCIATED CONTENT

### Supporting Information

Synthetic procedures, characterization data, details on binding studies, details on computational studies, X-ray data, NMR spectra. This material is available free of charge via the Internet at http://pubs.acs.org.

## AUTHOR INFORMATION


### Corresponding Author

diederich@org.chem.ethz.ch


### Notes

The authors declare no competing financial interest.

## ACKNOWLEDGMENTS

This work was supported by a grant from the Swiss National Science Foundation (SNF). I.P. acknowledges the receipt of a fellowship from the Fonds der Chemischen Industrie. J.M. and D.K. were funded by the Fond za Mlade Talente Republike Srbije. C.G. acknowledges the receipt of a fellowship from the Studienstiftung des deutschen Volkes.

## REFERENCES


(1) (a) Balzani, V.; Credi, A.; Raymo, F. M.; Stoddart, J. F. *Angew. Chem., Int. Ed.* **2000**, *39*, 3348. (b) Moonen, N.; Flood, A. H.; Fernández, J. M.; Stoddart, J. F. *Top. Curr. Chem.* **2005**, *262*, 99. (c) Browne, W. R.; Feringa, B. L. *Nature Nanotechnol.* **2006**, *1*, 25. (d) Kay, E. R.; Leigh, D. A.; Zerbetto, F. *Angew. Chem., Int. Ed.* **2007**, *46*, 72. (e) Coskun, A.; Banaszak, M.; Astumian, R. D.; Stoddart, J. F.; Grzybowski, B. A. *Chem. Soc. Rev.* **2011**, *41*, 19.

(2) (a) Moran, J. R.; Karbach, S.; Cram, D. J. *J. Am. Chem. Soc.* **1982**, *104*, 5826. (b) Moran, J. R.; Ericson, J. L.; Dalcanale, E.; Bryant, J. A.; Knobler, C. B.; Cram, D. J. *J. Am. Chem. Soc.* **1991**, *113*, 5707.

(3) Azov, V. A.; Beeby, A.; Cacciarini, M.; Cheetham, A. G.; Diederich, F.; Frei, M.; Gimzewski, J. K.; Gramlich, V.; Hecht, B.; Jaun, B.; Latychevskaia, T.; Lieb, A.; Lill, Y.; Marotti, F.; Schlegel, A.; Schlittler, R. R.; Skinner, P. J.; Seiler, P.; Yamakoshi, Y. *Adv. Funct. Mater.* **2006**, *16*, 147.

(4) Stimuli-responsive guest release has also been demonstrated in metallosupramolecular systems, see: (a) Mal, P.; Schultz, D.; Beyeh, K.; Rissanen, K.; Nitschke, J. R. *Angew. Chem., Int. Ed.* **2008**, *47*, 8297. (b) Han, M.; Michel, R.; He, B.; Chen, Y.-S.; Stalke, D.; John, M.; Clever, G. H. *Angew. Chem., Int. Ed.* **2012**, *52*, 1319. (c) Lewis, J. E. M.; Gavey, E. L.; Cameron, S. A.; Crowley, J. D. *Chem. Sci.* **2012**, *3*, 778.

(5) (a) Azov, V. A.; Jaun, B.; Diederich, F. *Helv. Chim. Acta* **2004**, *87*, 449. (b) Roncucci, P.; Pirondini, L.; Paderni, G.; Massera, C.; Dalcanale, E.; Azov, V. A.; Diederich, F. *Chem.—Eur. J.* **2006**, *12*, 4775.

(6) (a) Skinner, P. J.; Cheetham, A. G.; Beeby, A.; Gramlich, V.; Diederich, F. *Helv. Chim. Acta* **2001**, *84*, 2146. (b) Gottschalk, T.; Jarowski, P. D.; Diederich, F. *Tetrahedron* **2008**, *64*, 8307. (c) Gottschalk, T.; Jaun, B.; Diederich, F. *Angew. Chem., Int. Ed.* **2007**, *46*, 260.

(7) (a) Frei, M.; Marotti, F.; Diederich, F. *Chem. Commun.* **2004**, 1362. (b) Durola, F.; Rebek, J., Jr. *Angew. Chem., Int. Ed.* **2010**, *49*, 3189.

(8) Berryman, O. B.; Sather, A. C.; Rebek, J., Jr. *Chem. Commun.* **2010**, *47*, 656.

(9) (a) Pochorovski, I.; Boudon, C.; Gisselbrecht, J.-P.; Ebert, M.-O.; Schweizer, W. B.; Diederich, F. *Angew. Chem., Int. Ed.* **2012**, *51*, 262. (b) Pochorovski, I.; Ebert, M.-O.; Gisselbrecht, J.-P.; Boudon, C.; Schweizer, W. B.; Diederich, F. *J. Am. Chem. Soc.* **2012**, *134*, 14702.

(10) (a) Schierbaum, K. D.; Weiss, T.; Vanvelzen, E. U. T.; Engbersen, J. F. J.; Reinhoudt, D. N.; Gopel, W. *Science* **1994**, *265*, 1413. (b) Vanvelzen, E. U. T.; Engbersen, J. F. J.; Reinhoudt, D. N. *J. Am. Chem. Soc.* **1994**, *116*, 3597. (c) Huisman, B. H.; Rudkevich, D. M.; van Veggel, F. C. J. M.; Reinhoudt, D. N. *J. Am. Chem. Soc.* **1996**, *118*, 3523. (d) Schonherr, H.; Beulen, M. W. J.; Bugler, J.; Huskens, J.; van Veggel, F. C. J. M.; Reinhoudt, D. N.; Vancso, G. J. *J. Am. Chem. Soc.* **2000**, *122*, 4963. (e) Yamakoshi, Y.; Schlittler, R. R.; Gimzewski, J. K.; Diederich, F. *J. Mater. Chem.* **2001**, *11*, 2895. (f) Tsoi, S.; Griva, I.;

Trammell, S. A.; Blum, A. S.; Schnur, J. M.; Lebedev, N. *Acs Nano* **2008**, *2*, 1289. (g) Kim, H. J.; Lee, M. H.; Mutihac, L.; Vicens, J.; Kim, J. S. *Chem. Soc. Rev.* **2012**, *41*, 1173.
(11) (a) Rudkevich, D. M.; Hilmersson, G.; Rebek, J., Jr. *J. Am. Chem. Soc.* **1998**, *120*, 12216. (b) Rudkevich, D. M.; Hilmersson, G.; Rebek, J., Jr. *J. Am. Chem. Soc.* **1997**, *119*, 9911.
(12) Laurence, C.; Graton, J.; Berthelot, M.; Besseau, F.; Le Questel, J.-Y.; Luçon, M.; Ouvrard, C.; Planchat, A.; Renault, E. *J. Org. Chem.* **2010**, *75*, 4105.
(13) For an earlier communication on cavitand **6**, see reference 9b.
(14) An analogous basket equipped with $NBu_2$ instead of $NOct_2$ groups (reported in reference 9b) exhibited poor solubility in the reduced cavitand state. The $NOct_2$ groups significantly improve the solubility, allowing binding studies to be performed with ox-**7** and red-**7**.
(15) Tucci, F. C.; Rudkevich, D. M.; Rebek, J., Jr. *Chem.—Eur. J.* **2000**, *6*, 1007.
(16) Zhang, M.; Tsao, H. N.; Pisula, W.; Yang, C.; Mishra, A. K.; Müllen, K. *J. Am. Chem. Soc.* **2007**, *129*, 3472.
(17) Neto, B. A. D.; Lopes, A. S.; Wüst, M.; Costa, V. E. U.; Ebeling, G.; Dupont, J. *Tetrahedron Lett.* **2005**, *46*, 6843.
(18) Romer, D. R. *J. Heterocycl. Chem.* **2009**, *46*, 317.
(19) Serpell, C. J.; Kilah, N. L.; Costa, P. J.; Félix, V.; Beer, P. D. *Angew. Chem., Int. Ed.* **2010**, *49*, 5322.
(20) Gdaniec, M.; Bensemann, I.; Polonski, T. *Acta Crystallogr., Sect. C* **2004**, *60*, o215.
(21) Allison, C. G.; Chambers, R. D.; MacBride, J. A. H.; Musgrave, W. K. R. *J. Chem. Soc. C* **1970**, 1023.
(22) Martinelli, J. R.; Watson, D. A.; Freckmann, D. M. M.; Barder, T. E.; Buchwald, S. L. *J. Org. Chem.* **2008**, *73*, 7102.
(23) (a) Castro, P. P.; Zhao, G.; Masangkay, G. A.; Hernandez, C.; Gutierrez-Tunstad, L. M. *Org. Lett.* **2004**, *6*, 333. (b) Azov, V. A.; Diederich, F.; Lill, Y.; Hecht, B. *Helv. Chim. Acta* **2003**, *86*, 2149.
(24) This strategy was inspired by a report from Cram and co-workers, in which the fluorine atoms of a difluoropyrazine-substituted velcrand were substituted by *N*-, *O*, and *S*-nucleophiles: Cram, D. J.; Choi, H. J.; Bryant, J. A.; Knobler, C. B. *J. Am. Chem. Soc.* **1992**, *114*, 7748.
(25) The $^1$H NMR spectra of ox-**7** and red-**7** are shown in Figures S14 and S15 in the Supporting Information.
(26) For detailed information on computational studies, see section 3 of the Supporting Information.
(27) (a) Riley, K. E.; Platts, J. A.; Řezáč, J.; Hobza, P.; Hill, J. G. *J. Phys. Chem. A* **2012**, *116*, 4159. (b) Jackson, N. E.; Savoie, B. M.; Kohlstedt, K. L.; Olvera de la Cruz, M.; Schatz, G. C.; Chen, L. X.; Ratner, M. A. *J. Am. Chem. Soc.* **2013**, *135*, 10475.
(28) Further evidence for intermolecular associations is provided by the very broad IR absorption bands corresponding the OH groups in the solution state ($CDCl_3$) IR spectra of compounds red-**4** and red-**5**.
(29) For example, drying the cavitand at high vacuum for 30 d was not sufficient to remove residual THF: $^1$H NMR revealed that 1.1 equiv of THF was still present in the cavitand sample. Even after coevaporation with mesitylene-$d_{12}$ and subsequent drying at high vacuum, 0.4 equiv of THF still remained in the sample.
(30) Hornung, J.; Fankhauser, D.; Shirtcliff, L. D.; Praetorius, A.; Schweizer, W. B.; Diederich, F. *Chem.—Eur. J.* **2011**, *17*, 12362.
(31) For more details, see section 4 of the Supporting Information.
(32) (a) Santamaria, J.; Martin, T.; Hilmersson, G.; Craig, S. L.; Rebek, J., Jr. *Proc. Natl. Acad. Sci. U.S.A.* **1999**, *96*, 8344. (b) Craig, S. L.; Lin, S.; Chen, J.; Rebek, J., Jr. *J. Am. Chem. Soc.* **2002**, *124*, 8780. (c) Davis, A. V.; Raymond, K. N. *J. Am. Chem. Soc.* **2005**, *127*, 7912. (d) Pluth, M. D.; Raymond, K. N. *Chem. Soc. Rev.* **2007**, *36*, 161. (e) Rieth, S.; Hermann, K.; Wang, B.-Y.; Badjic, J. D. *Chem. Soc. Rev.* **2011**, *40*, 1609.
(33) (a) Warmuth, R.; Yoon, J. *Acc. Chem. Res.* **2001**, *34*, 95. (b) Quan, M. L.; Cram, D. J. *J. Am. Chem. Soc.* **1991**, *113*, 2754.